

**TITLE PAGE**

**Clearance and Biodistribution of Liposomally-Encapsulated Nitroxides: a Model for Targeted Delivery of Electron Paramagnetic Resonance Imaging Probes to Tumors**

Scott R. Burks<sup>1</sup>, Eric A. Legenzov, Gerald M. Rosen, and Joseph P.Y. Kao

Center for Biomedical Engineering and Technology and Center for EPR Imaging In Vivo Physiology, University of Maryland, Baltimore (SRB, EAL, GMR, JPYK)

Department of Physiology, University of Maryland, Baltimore (SRB, JPYK)

Department of Pharmaceutical Sciences, University of Maryland, Baltimore (GMR)

Laboratory of Origin (JPYK)

## **RUNNING TITLE PAGE**

### **Running Title: Clearance and Biodistribution of Nitroxides in Liposomes**

Address Correspondence to:

Joseph P.Y. Kao

725 W. Lombard St.

Baltimore, MD 21201

ph: 410-706-4167

fax: 410-706-8184

[jkao@umaryland.edu](mailto:jkao@umaryland.edu)

Number of Text Pages: 16

Number of Tables: 0

Number of Figures: 7

Number of References: 23

Words in Abstract: 197

Words in Introduction: 740

Words in Discussion: 814

Non-Standard Abbreviations: EPR, electron paramagnetic resonance; Hc7, HER2-overexpressing breast tumor cell derived from MCF7 cells

## ABSTRACT

Electron paramagnetic resonance (EPR) imaging using nitroxides as molecular probes is potentially a powerful tool for the detection and physiological characterization of micrometastatic lesions. Encapsulating nitroxides in anti-HER2 immunoliposomes at high concentrations, to take advantage of the “self-quenching” phenomenon of nitroxides, allows generation of robust EPR signals in HER2-overexpressing breast tumor cells with minimal background from indifferent tissues or circulating liposomes. We investigated the pharmacological properties *in vivo*, of nitroxides encapsulated in sterically-stabilized liposomes designed for long circulation times. We show that circulation times of nitroxides can be extended from hours to days; this increases the proportion of liposomes in circulation to enhance tumor targeting. Furthermore, nitroxides encapsulated in sterically-stabilized anti-HER2 immunoliposomes can be delivered to HER2-overexpressing tumors at micromolar concentrations, which should be imageable by EPR. Lastly, after administration *in vivo*, liposomally-encapsulated nitroxide signal also appears in the liver, spleen, and kidneys. While these organs are spatially distinct and would not hinder tumor imaging in our model, understanding nitroxide signal retention in these organs is essential for further improvements in EPR imaging contrast between tumors and other tissues. These results lay the foundation to use liposomally-delivered nitroxides and EPR imaging to visualize tumor cells *in vivo*.

## INTRODUCTION

The presence of micrometastatic breast lesions (< 2 mm) is correlated with poor clinical prognosis and decreased patient survival rate (Alix-Panabieres et al., 2007; Park et al., 2009). However, using current imaging methods to detect breast tumor micrometastases or monitor response to therapies remains a significant clinical challenge. Electron paramagnetic resonance (EPR) imaging is a magnetic resonance imaging modality that can image exogenous paramagnetic species, such as nitroxides, *in vivo*. If nitroxides can be selectively targeted to metastatic cells *in vivo*, EPR imaging becomes an attractive modality to image micrometastatic lesions. This is because nitroxides can be imaged with high contrast at micromolar concentrations and furthermore, can be chemically tailored to report cellular physiological information such as regional changes in pH (Halpern et al., 1989; Smirnov et al., 2004).

We have previously synthesized nitroxides that are suitable for cellular imaging: they are resistant to bioreduction and are retained in cells for sufficiently long periods to permit imaging (Rosen et al., 2005; Kao et al., 2007). We have further demonstrated that these nitroxides can be encapsulated in liposomes at high concentrations (>100 mM) and delivered to cells through endocytosis of liposomes (Burks et al., 2009). Liposomes encapsulating high concentrations of nitroxides are especially attractive carriers, because nitroxides exhibit the phenomenon of “self-quenching”, analogous to that of fluorophores, where spectral signals become greatly attenuated at high concentration. Therefore, intact liposomes in circulation are spectroscopically “dark” and thus contribute minimal background signal in imaging. After endocytosis by cells, liposomes are degraded, and the encapsulated nitroxides are released, and become greatly diluted,

into the intracellular volume. This dilution relieves self-quenching and restores the nitroxide spectral signal, making the cells appear “bright” and visible by EPR imaging. Moreover, this cell-activated, EPR signal-generating mechanism can be targeted to specific cells through the use of immunoliposomes. For example, we have demonstrated that anti-HER2 immunoliposomes can deliver high concentrations (~ 1 mM) of nitroxides selectively to HER2-overexpressing breast tumor cells *in vitro* (Burks et al., 2010b). With further improvements, it may be possible to generate high-contrast EPR images of these HER2-overexpressing cells *in vivo*.

Imaging tumor cells *in vivo* requires several additional considerations. Of primary concern are clearance mechanisms that limit efficacy of tumor targeting by liposomes. Liposomes must remain in circulation for a sufficient time to permit optimal tumor targeting and maximal delivery of EPR imaging agents. When liposomes are introduced into the circulation, opsonization promotes their rapid removal by the reticuloendothelial system (RES) (Liu and Liu, 1996; Yan et al., 2005). Liposomes can incorporate lipids that are conjugated to a high-molecular-weight (> 1 kDa) hydrophilic polymer, such as poly(ethyleneglycol) (PEG), to form sterically-stabilized liposomes. Such “PEGylated” liposomes differ from classical liposomes in their ability to evade clearance mechanisms and persist in the circulation for longer times (Woodle and Lasic, 1992).

The diameter of liposomes can drastically affect the rate of clearance from circulation. In general, clearance is faster for larger liposomes. An outer diameter of 100 nm is an optimal compromise for minimizing circulatory clearance while maximizing luminal capacity of the liposome (Harashima et al., 1994). With specific regard to *in vivo* tumor models, liposomes access tumors by extravasation into the interstitial space of the

tumor. Increasing the liposomal diameter beyond 100 nm hinders this process and greatly reduces liposome distribution in the tumor volume (Charrois and Allen, 2003).

In this study, we demonstrate the feasibility of visualizing HER2-overexpressing tumors *in vivo* with EPR imaging using anti-HER2 immunoliposomes to selectively deliver nitroxides. We have characterized nitroxide-encapsulating, sterically-stabilized, anti-HER2 immunoliposomes with regard to their persistence in circulation, stability, and the ultimate biodistribution of encapsulated nitroxides. We demonstrate that nitroxides in sterically-stabilized liposomes persist in circulation for days compared to hours with classical liposomes. Furthermore, these liposomes are highly stable in circulation and exhibit maximal self-quenching of encapsulated nitroxides; this minimizes background from the circulating liposomes. For tumor studies, we established xenograft tumors by inoculating mice with Hc7 cells, which are derived from the MCF-7 breast tumor cell line and engineered to overexpress HER2 (for cellular characterization see (Burks et al., 2010b)). We demonstrate that through targeted delivery of immunoliposome-encapsulated nitroxides, Hc7 xenograft tumors can accumulate nitroxide at concentrations that should be sufficient to permit EPR imaging. Lastly, we have surveyed the biodistribution of nitroxides and measured the relative rates of nitroxide metabolism by the tumor and other tissues. This knowledge may guide the design and synthesis of novel nitroxides to create maximal image contrast in HER2-overexpressing tumors.

## **MATERIALS AND METHODS**

### *General Materials*

Unless otherwise noted, all chemicals were obtained from commercial vendors

and used without purification. Dipotassium (2,2,5,5-tetramethylpyrrolidin-1-oxyl-3-ylmethyl)amine-*N,N*-diacetate (nitroxide **1**) was synthesized as previously described (Rosen et al., 2005). 3-Carboxy-2,2,5,5-tetramethyl-1-pyrrolidinyloxyl (nitroxide **2**, Sigma Aldrich, St Louis, MO) was converted to the corresponding potassium salt by the addition of KOH. Nitroxide molecular structures are shown in Figure 1. Cell culture reagents and biochemicals were from Invitrogen (Carlsbad, CA) or Hyclone (ThermoFisher Scientific, Waltham, MA). Chromatography resins were from Pharmacia or GE Healthcare (Piscataway, NJ).

### *Cell Culture*

Hc7 cells were cultured at 37 °C under humidified atmosphere containing 5% CO<sub>2</sub>. Cells were maintained in Dulbecco's Modified Eagle Medium (DMEM) supplemented with 10% fetal bovine serum, 2 mM L-glutamine, 100 U/mL penicillin, 100 µg/mL streptomycin, and 5 µg/mL Hygromycin B.

### *EPR Spectroscopy*

EPR spectra were recorded on an X-band EPR spectrometer (model E-109, Varian Associates, Palo Alto, CA). Instrumental settings were as follows: microwave frequency, 9.55 GHz; microwave power, 20 mW; magnetic field center, 333.5 mT; time constant, 0.5 s; modulation frequency, 100 kHz; modulation amplitude, 0.05-0.2 mT. The magnetic field was scanned from 0.8 to 8 mT at a rate of 2.67 mT/min. Instrument control and data digitization were performed with EWWIN32 (Scientific Software Solutions, Plymouth, MI). Reported spectral intensity is the intensity of the center peak in the nitroxide triplet spectrum.

### *Animals*

All animal protocols were approved by the Institutional Animal Care and Use Committee at the University of Maryland, Baltimore. Female NIH Swiss or NOD SCID mice (6 – 10 wks, Harlan Laboratories, Indianapolis, IN) were used for experimentation. Mice were housed under positive pressure on an alternating 12-hr light/dark cycle and given free access to food and water. SCID mice were previously ovariectomized by the vendor. Isoflurane inhalant was used for anesthesia (2.5% in O<sub>2</sub> for induction, 2.0% in O<sub>2</sub> for maintenance). Euthanasia was performed by asphyxiation with CO<sub>2</sub> followed by cervical dislocation.

### *Liposome Preparation*

Classical, sterically-stabilized, and immunoliposomes were prepared as described previously (Burks et al., 2009; Burks et al., 2010b). Briefly, all liposomes were primarily composed of 1,2-distearoylphosphatidylcholine (DSPC) and cholesterol (Chol) at a molar ratio of 3 DSPC to 2 Chol. Sterically-stabilized liposomes also incorporated 5 mole-% ammonium 1,2-distearoyl-*sn*-glycero-3-phosphatidylethanolamine-*N*-[poly(ethylene-glycol)2000] (PEG-PE). The formulation of anti-HER2 immunoliposomes was identical to sterically-stabilized liposomes except for the inclusion of ammonium 1,2-distearoyl-*sn*-glycero-3-phosphatidylethanolamine-*N*-[maleimide-poly(ethyleneglycol)2000] (PEG-PE-maleimide) at 1 mole-% to link trastuzumab Fab' fragments. All lipids were from Avanti Polar Lipids (Alabaster, AL). All liposomes were prepared to have a mean outer diameter of 100 nm and encapsulated 150 mM nitroxide **1**.

### *Clearance of Nitroxide-Containing Liposomes*

NIH Swiss mice were placed in a restrainer (Braintree Scientific, Braintree, MA) and administered nitroxide **1** (25 nmol/g bw) via tail vein injection. Nitroxide was



encapsulated in classical liposomes or sterically-stabilized liposomes, or was used as free (unencapsulated) nitroxide in DPBS. Injection volumes were ~100  $\mu$ L. At various times, blood (~10  $\mu$ L) was collected into heparinized micro-hematocrit capillary tubes (ThermoFisher Scientific) and then diluted into 1 mL deionized H<sub>2</sub>O (resistivity = 18.3 M $\Omega$ -cm). Diluted blood samples were subjected to three freeze-thaw cycles to ensure lysis of liposomes. Samples were measured by EPR spectroscopy to determine nitroxide content. Each sample was also measured for plasma sodium content using a sodium-selective electrode (ThermoFisher Scientific), and nitroxide content was normalized to plasma sodium content. To determine self-quenching of liposome-encapsulated nitroxides in circulation, a blood sample (~25  $\mu$ L) was taken 24 hr after injection with sterically-stabilized liposomes and diluted into 450  $\mu$ L DBPS. The same sample was immediately measured by EPR spectroscopy before and after the addition of Triton X-100 (0.5% v/v).

#### *Establishing Hc7 xenografts*

At least 48 hr prior to inoculation with Hc7 cells, biodegradable, time-release estrogen pellets (2.5 mg/90 days, Innovative Research of America, Sarasota, FL) were subcutaneously implanted into the shoulders of SCID mice. Hc7 cells were cultured to ~90% confluence in 150 cm<sup>2</sup> culture flasks. Cells were washed thrice with Dulbecco's phosphate buffered saline (DPBS) and then removed from the flask by incubation at 37 °C in a solution containing 100 mM KCl, 50 mM sodium citrate (pH 7.0), and 0.5 mM disodium dihydrogen ethylenediaminetetraacetate (Na<sub>2</sub>H<sub>2</sub>EDTA). Collected cells were washed twice with DPBS and suspended in DPBS to a final concentration of  $2 \times 10^7$  cells/mL.  $2 \times 10^6$  cells were subcutaneously injected into each rear leg of a SCID mouse.

Each week, tumor sites were inspected for palpable tumors, and volume was determined using radial measurements performed with calipers. Tumors were measured in two dimensions, length and width, and volume ( $V$ ) was calculated by the formula  $V = \frac{4}{3}\pi r_1^2 r_2$  where  $r_1$  is one-half the smaller of the two tumor dimensions and  $r_2$  is one-half the larger dimension.

#### *Biodistribution of Nitroxide-Loaded Immunoliposomes and Uptake by Hc7 Tumors*

SCID mice bearing Hc7 xenograft tumors ( $> 200 \text{ mm}^3$ ) were administered anti-HER2 immunoliposomes containing 5 mole-% PEG-PE and encapsulating nitroxide **1** by tail vein injection. Mice received immunoliposomes at 25 nmoles nitroxide/g bw. At various times, mice were euthanized, placed on ice, and the vasculature was perfused with cold DPBS to displace blood. DPBS was pumped through a 27 G butterfly needle inserted into the left ventricle. Part of the right atrium was excised to allow drainage. Animals were perfused until clear saline emerged from the right atrium (~5 min). Tumors were then excised and weighed. Each sample was homogenized in 3 mL DPBS and sonicated for 30 sec. Tumor homogenates were measured by EPR spectroscopy for nitroxide content. Maximal tumor-associated nitroxide signal occurred 3 hr after injection (see Results). Therefore, to assess biodistribution of nitroxides at that time point, other SCID mice were injected with immunoliposomes and after 3 hr, liver, spleen, kidney, brain, lung, and muscle were harvested, weighed, and measured for nitroxide content by the same protocol as that for the tumors.

#### *Reduction of Nitroxides by Tissue Homogenates*

NIH Swiss mice were euthanized and kidney, liver, and spleen were harvested. Tissues were washed with DPBS and maintained on ice. Tissue samples were weighed

and then homogenized in DPBS (0.210 mg tissue / mL DPBS). Homogenates were pulse-sonicated for 10 s at 20 W (Sonifier 450, Branson Ultrasonics Corporation, Danbury, CT). At time zero, 5  $\mu$ L of a stock solution of nitroxide **2** (40 mM in H<sub>2</sub>O) was added to 400  $\mu$ L of the freshly-prepared homogenate (final nitroxide concentration of 500  $\mu$ M). The mixture was immediately transferred to an EPR cuvette that had previously been purged with N<sub>2</sub> and sealed. Nitroxide reduction proceeded at room temperature (23 °C), and at various times, EPR spectra were acquired. To measure nitroxide reduction by Hc7 tumors, Hc7 cells were used in place of dissected tumors because tumors sometimes showed necrotic interiors, which would have given less consistent bio-reduction. Cultured Hc7 cells were detached from culture flasks by treatment with trypsin and centrifuged (805  $\times$  g). The pellet was weighed and suspended in DPBS at the same concentration as harvested tissues. Cells were lysed by sonication for 60 sec in a bath sonicator (80 W power; Laboratory Supplies Company, Hicksville, NY), and nitroxide reduction was measured following the same procedure as that used for other tissues. Each time course was measured in duplicate and plotted points are averaged measurements.

### *Data Analyses*

OriginPro 8 (OriginLabs, Northampton, MA) and CorelDraw X4 (Corel Inc, Mountain View, CA) were used for data analyses and presentation. Mean values are plotted and error bars represent standard deviation. One-way ANOVAs were used to determine significance among data sets. Differences above the 95% confidence interval ( $p < 0.05$ ) were considered significant. Bonferroni tests were used for post-hoc analyses. Exponential time courses were fit with first-order exponential functions. For nitroxide reduction measurements, irregular measurement intervals in the repeated measurements

were regularized by interpolation after fitting a 2<sup>nd</sup>-degree polynomial function to the three nearest points. The initial value (at time zero) of each time course was extrapolated by linear least-squares analysis performed on the first three data points. Data points in each curve were then normalized to the extrapolated initial value.

## RESULTS

### *Circulatory Clearance of Nitroxide-Containing Liposomes*

To assess the improvement in circulatory retention of sterically-stabilized liposomes, mice were given classical liposomes (lacking PEG-PE) or sterically-stabilized liposomes (containing 5 mole-% PEG-PE) that both encapsulated 150 mM nitroxide **1**. At various times, blood samples were drawn from the mice, and intact liposomes in the blood were lysed by repeated freeze/thaw cycles; nitroxide content in each sample was then measured. Clearance results are summarized in Figure 2. The clearance time course of classical liposomes is best fit by a first-order exponential decay function having a time constant ( $\tau = t_{1/e}$ ) of  $6.9 \pm 1.1$  hr, which is equivalent to a half-life of  $t_{1/2} = 4.8 \pm 0.8$  hr ( $t_{1/2} = \ln 2 \times \tau$ ). Clearance is more than 95% complete after  $3\tau$ , or ~20 hr for classical liposomes. Sterically-stabilized liposomes, however, remained in circulation 2.3-fold longer ( $\tau = 16.0 \pm 3.2$  hr or  $t_{1/2} = 11.1 \pm 2.3$  hr). Thus, by incorporating PEG-PE into the liposomal formulation, even after 36 hr, greater than 10% of the injected nitroxide signal is still present in the circulation.

While background EPR signal in the circulation can be minimized by encapsulating quenched concentrations of nitroxides in liposomes, any nitroxide that has leaked from liposomes would become dequenched and thus contribute unwanted

background signal in the circulation. We expected signal from leaked nitroxides to be minimal because renal filtration should efficiently remove small ionic solutes such as nitroxide **1** from circulation. Indeed, when mice were injected with free nitroxide **1** (not encapsulated in liposomes), clearance was very rapid ( $\tau = 2.88 \pm 0.34$  min,  $t_{1/2} = 2.00 \pm 0.24$  min). Therefore, extra-liposomal nitroxide is unlikely to contribute significant background signal in the circulation.

Even though nitroxides leaked from circulating liposomes are cleared rapidly, a potential problem arises if liposomes lose sufficient nitroxide so that the spectroscopic signal of the nitroxides that remain entrapped becomes incompletely quenched. In this case, the circulating liposome itself would become the source of unwanted background signal. Analysis of blood collected 24 hr after injection with sterically-stabilized liposomes demonstrates that they are exceptionally stable *in vivo* (Fig 3). Blood samples were measured by EPR spectroscopy both before and after liposomal lysis. The robust post-lysis spectrum shows ~50-fold greater amplitude than the pre-lysis spectrum; this leads to three significant inferences. First, the robust post-lysis spectrum shows that a significant number of liposomes remain in circulation after 24 hr. Second, the minimal pre-lysis spectrum demonstrates that circulating liposomes have retained enough nitroxide to exhibit essentially complete quenching of the EPR signal. Third, the pre-lysis spectrum confirms what is shown in Figure 2: that if any nitroxide did escape the liposome, it was efficiently removed from the circulation and did not contribute a background signal.

Before *in vivo* tumor targeting experiments can be performed, Hc7 xenograft tumors must be generated. Hc7 cells were subcutaneously injected into both flanks of

SCID mice ( $n = 5$ ) and cell proliferation was stimulated with estrogen. Tumors were established at all injection sites ( $n = 10$ ). The tumors became palpable within 1 week and reached an average volume of  $300 \text{ mm}^3$  in  $< 2.5$  weeks (Fig 4A). At five weeks after implantation, the average tumor volume was almost  $2,000 \text{ mm}^3$  (representative mouse shown in Fig 4B).

EPR imaging of Hc7 tumors should be performed when accumulated nitroxide signal in the tumors is maximal. To investigate this, Hc7-tumor-bearing mice were administered anti-HER2 immunoliposomes encapsulating 150 mM nitroxide **1**. At various times, mice were euthanized and the vasculature was perfused with DPBS to remove circulating liposomes. Tumors ( $n = 5 - 8$ ) were excised at each time point, rapidly homogenized, and the tissue homogenate was immediately measured by EPR spectroscopy to determine tumor-associated nitroxide content. As shown in Figure 5, tumors accumulated maximal nitroxide ( $\sim 5 \text{ nmol/g}$ ) by 3 hr post-injection. The measured EPR signal persisted until 6 hr, and then declined. By 9 hr post injection, nitroxide signal decayed to approximately 35% of the maximum measured at 3 hr ( $\text{ANOVA}_{F_{4,26}} = 7.30$ ).

Knowing that Hc7 tumors reach peak EPR signal intensities by 3 hr, we measured the distribution of nitroxides in other tissues at that time and determined the nitroxide content associated with other tissues. Measureable nitroxide accumulated in tumor tissue at a concentration of  $\sim 5 \text{ nmole/g}$  at 3 hr post-injection (Fig 6). Organs that are associated with clearance of nitroxides and liposomes also accumulate measureable nitroxide content:  $\sim 10 \text{ nmol/g}$  in the kidneys,  $\sim 2.5 \text{ nmol/g}$  in the liver,  $\sim 30 \text{ nmol/g}$  in the spleen. Based on the weight of each organ, the fraction of the total injected dose of nitroxides that appears in each tissue is:  $\sim 2.0 \times 10^{-3} \%$  in the tumors,  $\sim 3.5 \times 10^{-3} \%$  in the kidneys,

$\sim 1.5 \times 10^{-3}$  % in the liver, and  $\sim 3.0 \times 10^{-3}$  % in the spleen. Other tissues that would not be expected to interact with liposomes, such as brain, muscle, and lungs, did not have any measureable nitroxide content.

Lastly, because nitroxides are susceptible to metabolism in tissue, the observed nitroxide signal in any tissue depends on both liposomal delivery to, and nitroxide metabolism by, that tissue. Therefore, we measured the relative rates of nitroxide signal decay in each tissue. Freshly-homogenized tissue was mixed with nitroxide and sealed in a cuvette under inert atmosphere; EPR signal intensity was monitored over 3 hr (Fig. 7). Not surprisingly, nitroxide signal disappeared most rapidly in the liver and kidney homogenates. After 3 hr, only 5% and 15% of the original nitroxide signal was detectable in the liver and kidney homogenates, respectively. In contrast, at the same time point, 50% of the nitroxide signal was still detectable in the spleen sample and  $\sim 65\%$  was measured in the Hc7 homogenate.

## DISCUSSION

We have demonstrated that administering sterically-stabilized anti-HER2 immunoliposomes encapsulating quenched concentrations of nitroxide **1** to mice bearing Hc7 tumors results in accumulation of nitroxide in the tumors. We have shown that encapsulation in sterically-stabilized liposomes enables nitroxides to remain in the circulation for days. Furthermore, these liposomes are sufficiently biostable to maintain essentially maximal quenching of the EPR signal of encapsulated nitroxides. Such stability is important for minimizing background signal in the circulation to make high-contrast imaging possible. We show that the nitroxide signal in Hc7 tumors was maximal

after 3 hr, which allows imaging studies to be conducted shortly after nitroxide administration. At that time point, tissues that are not expected to interact with the immunoliposomes (e.g., brain, lung, and muscle), showed no measurable nitroxide signal. Not surprisingly, organs that mediate clearance of nitroxides and liposomes (liver, kidney, and spleen) did accumulate nitroxide signal. Importantly, the total amount of nitroxide detected in tissues by 3 hr post-injection (<1% total nitroxide dose) is only a small fraction of what has been cleared from the circulation at that time (~20% total dose). The fact that these nitroxides are exceptionally resistant to bioreduction in the blood/plasma (Burks et al., 2009; Miyake et al., 2010), and further protected from metabolic degradation by being encapsulated in liposomes, implies the vast majority of cleared nitroxides are subjected to one of two fates: metabolic degradation by the liver and kidney (Figure 7) or possibly, excretion by the kidneys into the urine.

The biodistribution of nitroxides almost completely agrees with previous biodistribution measurements of  $^{67}\text{Ga}$  encapsulated in anti-HER2 immunoliposomes (Kirpotin et al., 2006). However, the quantities of tumor-associated nitroxide and  $^{67}\text{Ga}$  differ with respect to the amount in the liver and kidneys. Compared to nitroxides,  $^{67}\text{Ga}$  accumulated more in the liver but less in the kidney. This result is of interest because signal intensity differences between tissues facilitate differentiation of those tissues in imaging. Tumor-associated nitroxide signal is statistically similar to that associated with both liver and kidneys, whereas tumor-associated  $^{67}\text{Ga}$  is statistically different from that in the liver and kidneys. Conveniently in the current Hc7 model, the tumors are spatially distinct from the liver and kidneys; this would enable the different tissues to be discerned readily in images.



In the liver, which is highly metabolically active, nitroxides are reduced to the corresponding hydroxylamines, which do not produce EPR signal (Kocherginsky and Swartz, 1995; Rosen and Rauckman, 1977). Although the nitroxides used in this study were specifically designed to resist bioreduction (Keana et al., 1987; Halpern et al., 1996), bioreduction can still occur. This could account for relatively less nitroxide being found in the liver compared to  $^{67}\text{Ga}$ , whose clearance from the liver occurs over days to months (Dudley et al., 1949). The relationship between molecular structure and susceptibility to reduction has been extensively studied in nitroxides (Keana et al., 1987). If nitroxides could be designed to increase reduction in the liver without a corresponding change in tumor tissue, then EPR signal from liver can be markedly reduced. This would enable tumor and liver to be distinguished more readily on the basis of signal intensity.

Nitroxides and  $^{67}\text{Ga}$  also accumulate differently in the kidneys. Administration through immunoliposomes results in relatively more nitroxide than  $^{67}\text{Ga}$  in the kidneys. One potential explanation is partial leakage of nitroxides from circulating liposomes, which previous studies have suggested is a possibility (Burks et al., 2009). Such leaked nitroxides, being small anions, would be filtered by, and thus appear in, the kidneys. A potential solution would be to modify the nitroxide molecular structure to improve entrapment within liposomes. The most straightforward approach would be to increase the number of ionic groups on the nitroxide.

The amount of nitroxide observed in tumors after 3 hr is  $\sim 5$  nmole/g—corresponding to a concentration of  $\sim 5$   $\mu\text{M}$ . Our preliminary imaging studies of Hc7 tumors and previous studies (Burks et al., 2009; Burks et al., 2010b) suggest this concentration should be just visible in reconstructed images which have the benefit of

signal averaging to increase signal-to-noise ratio (SNR). A number of recent advances in EPR imaging technology should markedly improve the ease of tumor imaging with nitroxides delivered through immunoliposomes. First, the intrinsic SNR of nitroxides can be improved by more than 7-fold through systematic  $^{15}\text{N}$  and  $^2\text{H}$  isotopic substitution in the nitroxides (Burks et al., 2010a). Additionally, the development of rapid-scan continuous-wave acquisition permits megagauss-per-minute scanning by the imaging spectrometer—a five-orders-of-magnitude improvement over current scanning speeds. This should afford markedly improved SNR through signal averaging (Quine et al., 2010; Tseitlin et al., 2010).

In total, our results lay the groundwork to use sterically-stabilized immunoliposomes to deliver nitroxides to HER2-overexpressing breast tumors *in vivo*. By characterizing the pharmacological properties of nitroxides in liposomes, we have demonstrated that only modest improvements are required to enable high-contrast EPR images of Hc7 tumors *in vivo*. These studies are currently underway in our laboratory.

## **AUTHORSHIP CONTRIBUTIONS**

*Participated in research design:* Burks, Rosen, Kao

*Conducted Experiments:* Burks, Legenzov, Kao

*Contributed new reagents or analytic tools:* Rosen

*Performed data analyses:* Burks, Kao

*Wrote or contributed to the writing of the manuscript:* Burks, Rosen, Kao

## REFERENCES

Alix-Panabieres C, Muller V and Pantel K (2007) Current status in human breast cancer micrometastasis. *Curr Opin Oncol* **19**:558-563.

Burks SR, Bakhshai J, Makowsky MA, Muralidharan S, Tsai P, Rosen GM and Kao JP (2010a) (2)H,(15)N-substituted nitroxides as sensitive probes for electron paramagnetic resonance imaging. *J Org Chem* **75**:6463-6467.

Burks SR, Barth ED, Halpern HJ, Rosen GM and Kao JP (2009) Cellular uptake of electron paramagnetic resonance imaging probes through endocytosis of liposomes. *Biochim Biophys Acta* **1788**:2301-2308.

Burks SR, Macedo LF, Barth ED, Tkaczuk KH, Martin SS, Rosen GM, Halpern HJ, Brodie AM and Kao JP (2010b) Anti-HER2 immunoliposomes for selective delivery of electron paramagnetic resonance imaging probes to HER2-overexpressing breast tumor cells. *Breast Cancer Res Treat* **124**:121-131.

Charrois GJ and Allen TM (2003) Rate of biodistribution of STEALTH liposomes to tumor and skin: influence of liposome diameter and implications for toxicity and therapeutic activity. *Biochim Biophys Acta* **1609**:102-108.

Dudley HC, Maddox GE and La Rue HC (1949) Studies of the metabolism of gallium. *J Pharmacol Exp Ther* **96**:135-138.

Halpern HJ, Peric M, Yu C, Barth ED, Chandramouli GV, Makinen MW and Rosen GM (1996) In vivo spin-label murine pharmacodynamics using low-frequency electron paramagnetic resonance imaging. *Biophys J* **71**:403-409.

Halpern HJ, Spencer DP, Vanpolen J, Bowman MK, Nelson AC, Dowe EM and Teicher BA (1989) Imaging Radio-Frequency Electron-Spin-Resonance Spectrometer with High-Resolution and Sensitivity for In vivo Measurements. *Review of Scientific Instruments* **60**:1040-1050.

Harashima H, Sakata K, Funato K and Kiwada H (1994) Enhanced hepatic uptake of liposomes through complement activation depending on the size of liposomes. *Pharm Res* **11**:402-406.

Kao JP, Barth ED, Burks SR, Smithback P, Mailer C, Ahn KH, Halpern HJ and Rosen GM (2007) Very-low-frequency electron paramagnetic resonance (EPR) imaging of nitroxide-loaded cells. *Magn Reson Med* **58**:850-854.

Keana JF, Pou S and Rosen GM (1987) Nitroxides as potential contrast enhancing agents for MRI application: influence of structure on the rate of reduction by rat hepatocytes, whole liver homogenate, subcellular fractions, and ascorbate. *Magn Reson Med* **5**:525-536.

Kirpotin DB, Drummond DC, Shao Y, Shalaby MR, Hong K, Nielsen UB, Marks JD, Benz CC and Park JW (2006) Antibody targeting of long-circulating lipidic nanoparticles

does not increase tumor localization but does increase internalization in animal models.

*Cancer Res* **66**:6732-6740.

Kocherginsky N and Swartz HM (1995) Metabolism of nitroxides and their products in cells, in *Nitroxide spin labels: reactions in biology and chemistry* pp 126-135, CRC Press, Boca Raton, FL.

Liu F and Liu D (1996) Serum independent liposome uptake by mouse liver. *Biochim Biophys Acta* **1278**:5-11.

Miyake M, Burks SR, Weaver J, Tsai P, Liu W, Bigio D, Bauer KS, Liu KJ, Rosen GM and Kao JP (2010) Comparison of two nitroxide labile esters for delivering electron paramagnetic resonance probes into mouse brain. *J Pharm Sci* **99**:3594-3600

Park D, Karesen R, Naume B, Synnestvedt M, Beraki E and Sauer T (2009) The prognostic impact of occult nodal metastasis in early breast carcinoma. *Breast Cancer Res Treat* **118**:57-66.

Quine RW, Rinard GA, Eaton SS and Eaton GR (2010) Quantitative rapid scan EPR spectroscopy at 258 MHz. *J Magn Reson* **205**:23-27.

Rosen GM, Burks SR, Kohr MJ and Kao JP (2005) Synthesis and biological testing of aminoxyls designed for long-term retention by living cells. *Org Biomol Chem* **3**:645-648.

Rosen GM and Rauckman EJ (1977) Formation and reduction of a nitroxide radical by liver-microsomes. *Biochem Pharmacol* **26**:675-678

Smirnov AI, Ruuge A, Reznikov VA, Voinov MA and Grigor'ev IA (2004) Site-directed electrostatic measurements with a thiol-specific pH-sensitive nitroxide: differentiating local pK and polarity effects by high-field EPR. *J Am Chem Soc* **126**:8872-8873.

Tseitlin M, Quine RW, Rinard GA, Eaton SS and Eaton GR (2010) Combining absorption and dispersion signals to improve signal-to-noise for rapid-scan EPR imaging. *J Magn Reson* **203**:305-310.

Woodle MC and Lasic DD (1992) Sterically stabilized liposomes. *Biochim Biophys Acta* **1113**:171-199.

Yan X, Scherphof GL and Kamps JA (2005) Liposome opsonization. *J Liposome Res* **15**:109-139.

## FOOTNOTES

This work was supported by the National Institutes Health [Grants GM-56481, P41-EB-2034]

<sup>1</sup>Current affiliation: Frank Laboratory and Imaging Sciences Training Program, Clinical Center, National Institutes of Health, Bethesda, MD



## FIGURE LEGENDS

Figure 1. Molecular structures of nitroxides used in the present study.

Figure 2. Clearance of free and liposomally-encapsulated nitroxides. Circulatory clearance of nitroxide **1** was measured after iv injection in mice ( $n = 6$ ). Injections were of nitroxide **1** encapsulated in sterically-stabilized liposomes (squares; solid curve is single-exponential fit), encapsulated in classical liposomes (circles; dashed curve), or free in solution (triangles; dotted curve). Addition of 5 mole-% PEG-PE to form sterically-stabilized liposomes increases the exponential lifetime ( $t_{1/e}$ ) of nitroxides in circulation from  $\sim 7$  hr to 16 hr. Unencapsulated nitroxide is cleared from circulation with an exponential lifetime of  $\sim 3$  min. Where not shown, error bars are smaller than symbols.

Figure 3. Liposomally-encapsulated nitroxides exhibit self-quenching after 24 hr in circulation. Blood was drawn from mice 24 hr after iv injection of sterically-stabilized liposomes encapsulating 150 mM nitroxide **1**. The pre-lysis EPR spectrum (red trace) shows minimal nitroxide signal. However, after liposomes in the same blood sample were lysed and the EPR spectrum was recorded again (black trace), robust nitroxide signal was observed. This verifies the presence of intact liposomes that still encapsulate high concentrations of nitroxide, as well as the absence of leaked nitroxides in circulation.

Figure 4. Hc7 xenograft model. SCID mice ( $n = 5$ ) were subcutaneously inoculated with a suspension of Hc7 cells, and tumor growth was stimulated with estrogen. The tumor growth curve is shown in (A); the smooth curve is a least-squared fit of the data to a single-exponential function; the dashed line marks the time at which average tumor volume reached  $300 \text{ mm}^3$ . Where not shown, error bars are smaller than

symbols. A representative mouse 5 weeks after inoculation is shown in (B); arrows mark the tumors on each side of the mouse.

Figure 5. Tumor-associated nitroxide EPR signal. SCID mice bearing Hc7 tumors ( $n = 5 - 8$ ) were intravenously injected with anti-HER2 immunoliposomes containing 5 mole-% PEG and encapsulating nitroxide **1**, and nitroxide signal accumulation in the tumors was monitored. Maximal signal is reached by 3 hr, persists through 6 hr, and declines afterward. Statistical significance is indicated by asterisks and diamonds. Groups marked by identical symbols are statistically similar to one and other and are different from groups marked by other symbols. ANOVA  $F_{4,26} = 7.30$ .

Figure 6. Biodistribution of nitroxides 3 hr after injection of nitroxide **3** encapsulated in anti-HER2 immunoliposomes. SCID mice bearing Hc7 tumors ( $n = 4$ ) were intravenously injected with immunoliposomes encapsulating 150 mM nitroxide **1**. After 3 hr, mice were euthanized and the vasculature was perfused with saline. Tissues were harvested, homogenized, and analyzed for nitroxide content. Tumor, kidney, spleen, and liver tissue accumulated nitroxide to varying extents, while brain, muscle, and lung had no detectable nitroxide (indicated by n.d.). Statistical significance is indicated by asterisks, daggers, and diamonds. Groups marked by identical symbols are statistically similar to one and other and are different from groups marked by other symbols. ANOVA  $F_{6,28} = 16.13$ .

Figure 7. Decay of nitroxide signal in different tissues. Nitroxide **2** was added to freshly-prepared tissue homogenates under inert atmosphere and EPR signal intensity was monitored over 180 min. Nitroxide signal disappeared relatively quickly from the liver and kidney samples. Only 5% and 15% of the original nitroxide signal was

detectable in the liver and kidney sample, respectively, after 180 min. Signal was more persistent in the spleen and Hc7 samples, which retained 50% and 65%, respectively, of the original nitroxide signal after 180 min. Measurements were repeated twice in random order and each point is the average of two measurements.

Figure 1

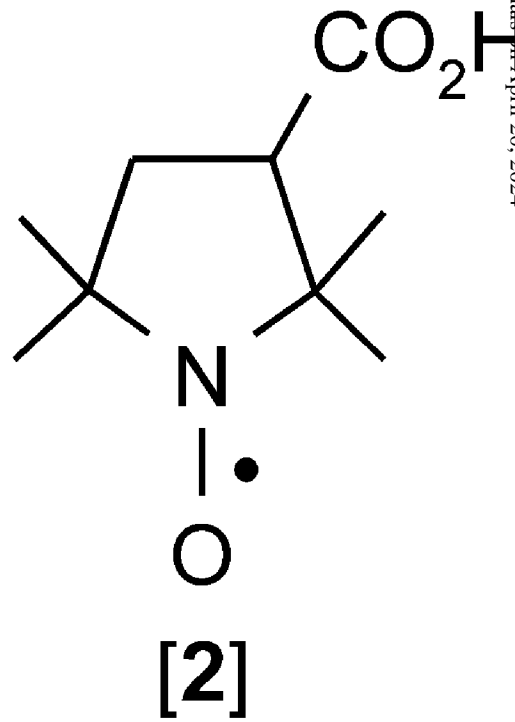
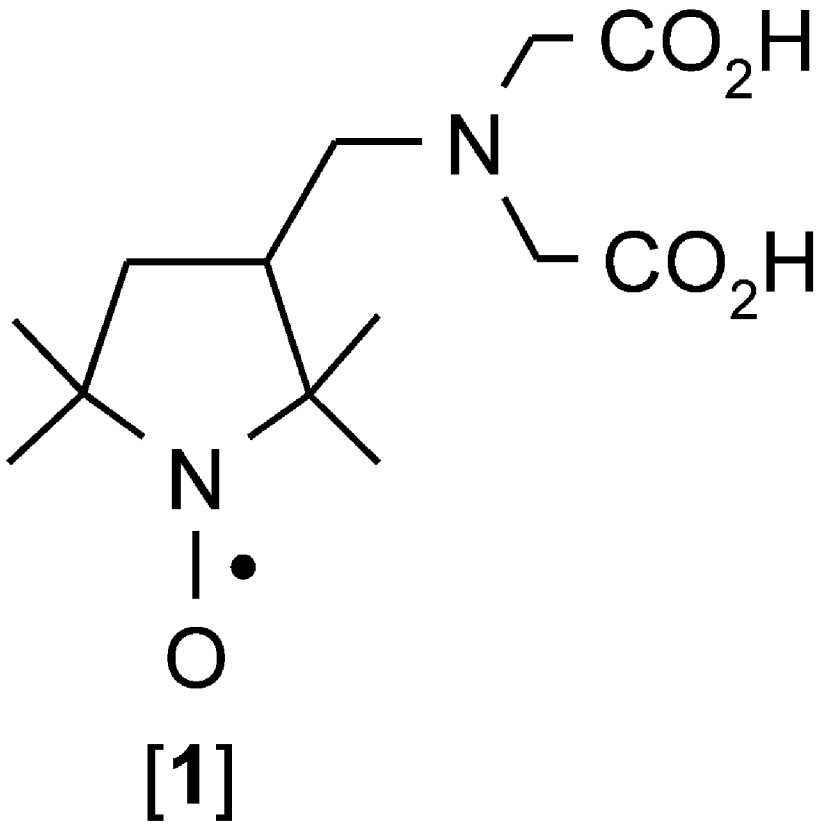


Figure 2

Fractional Circulating Nitroxide

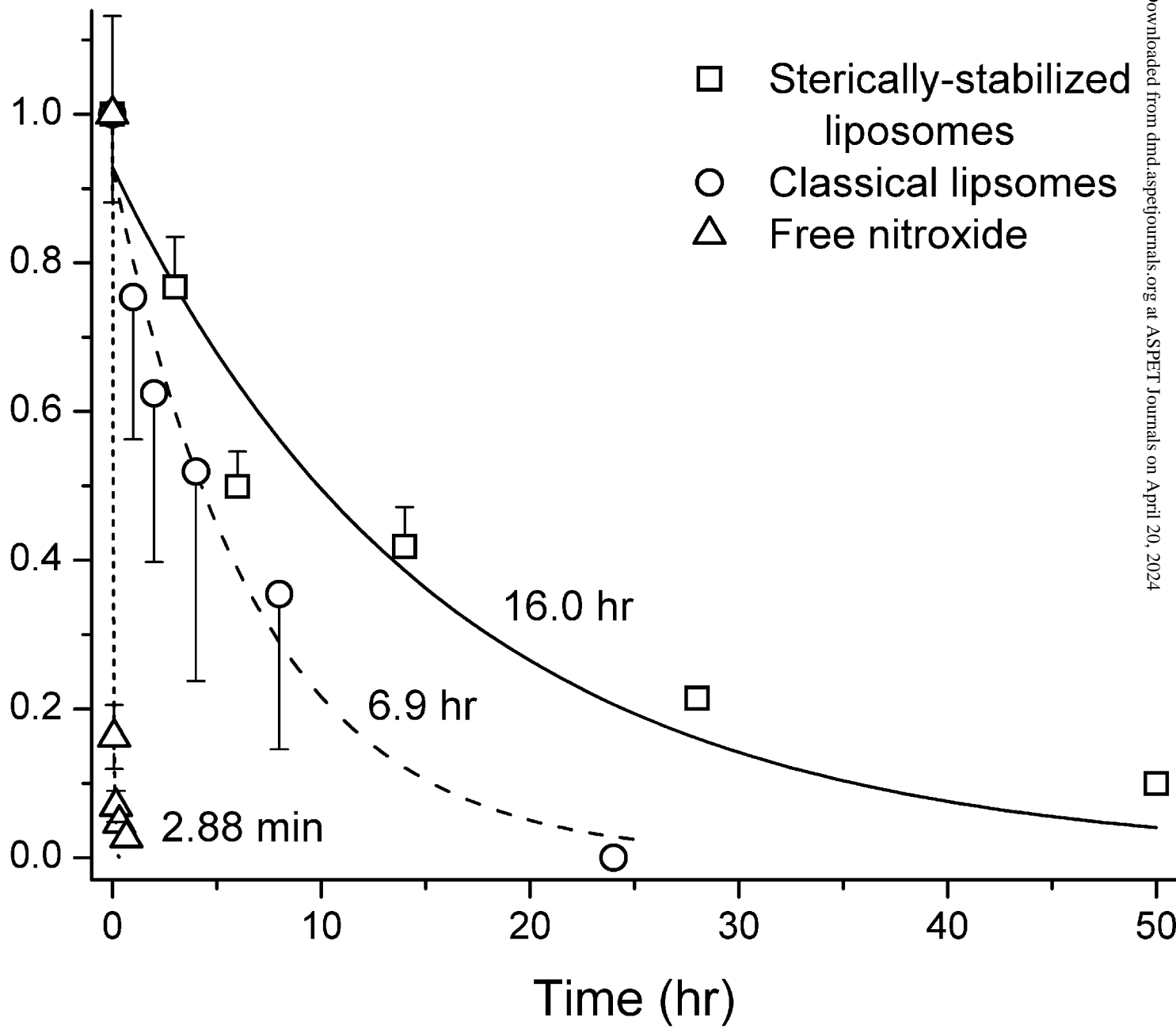


Figure 3

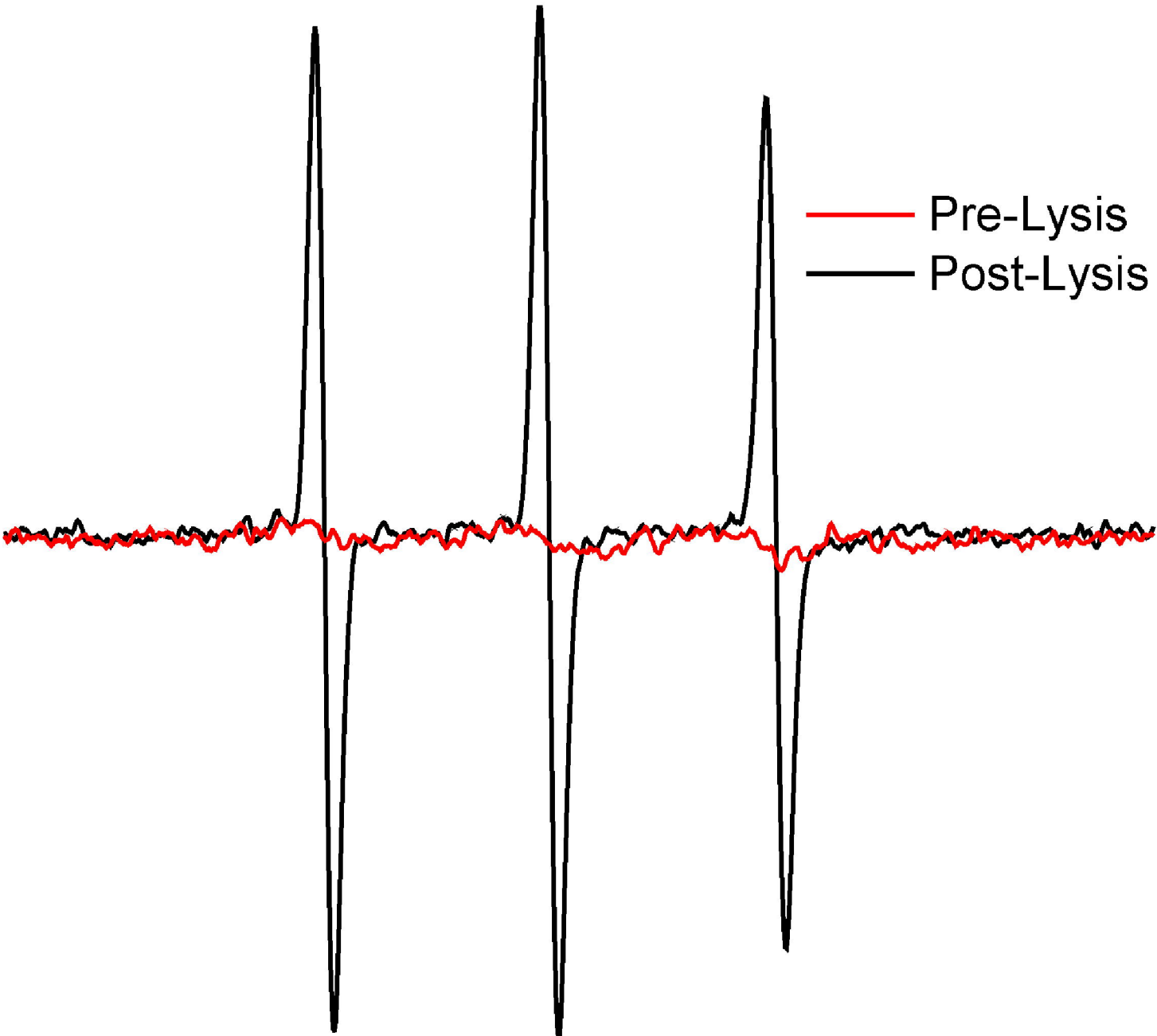


Figure 4

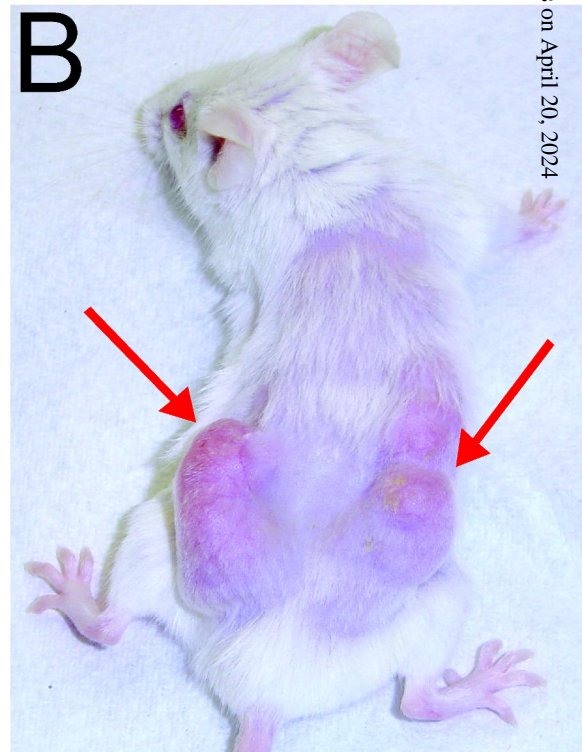
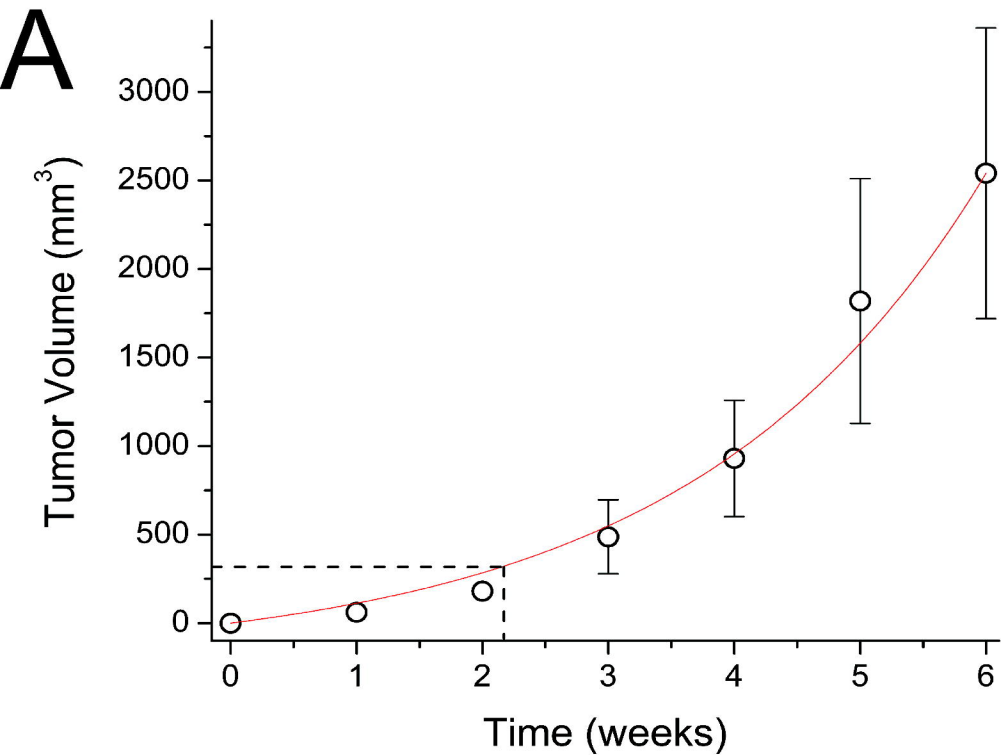


Figure 5

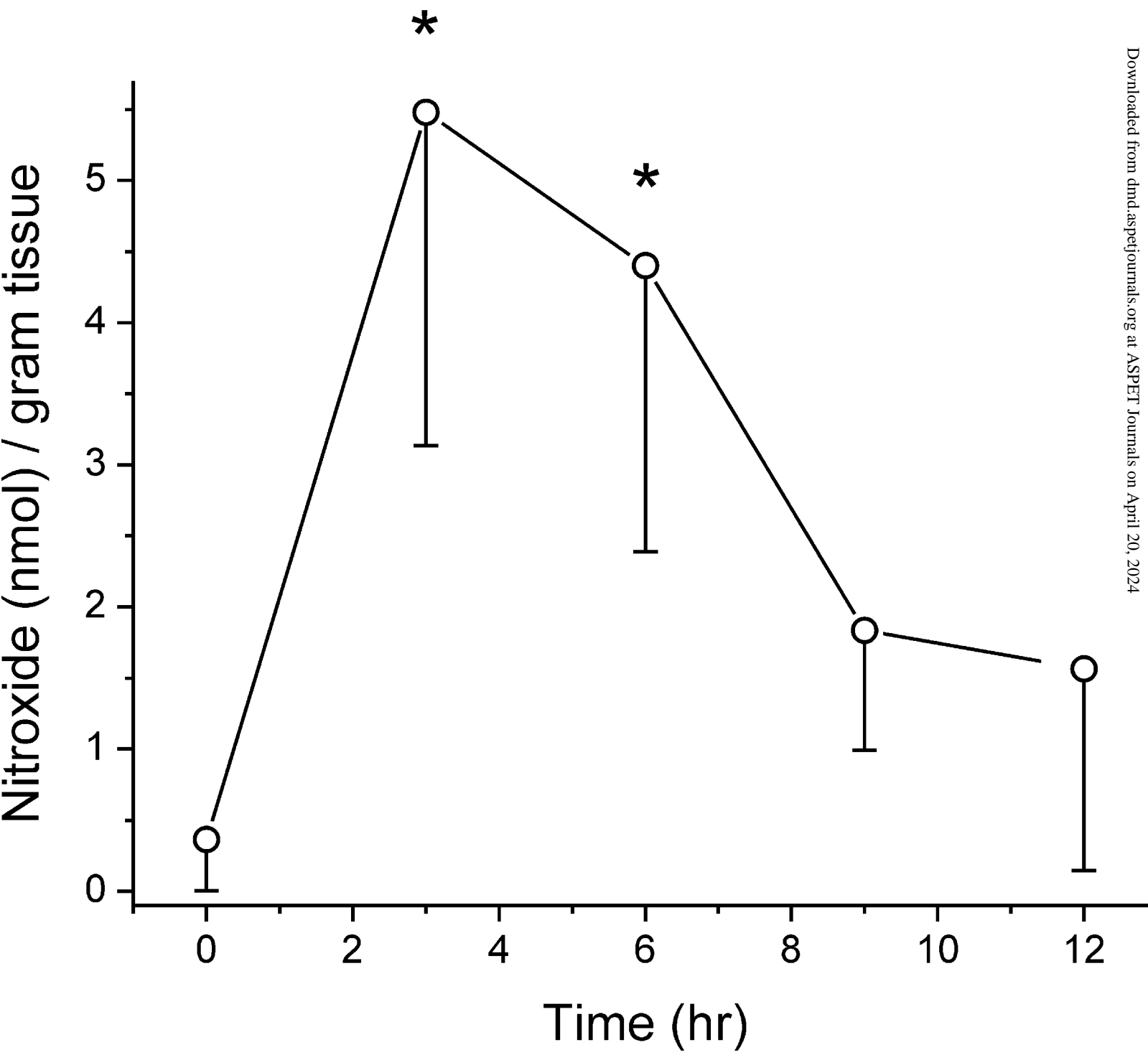




Figure 6

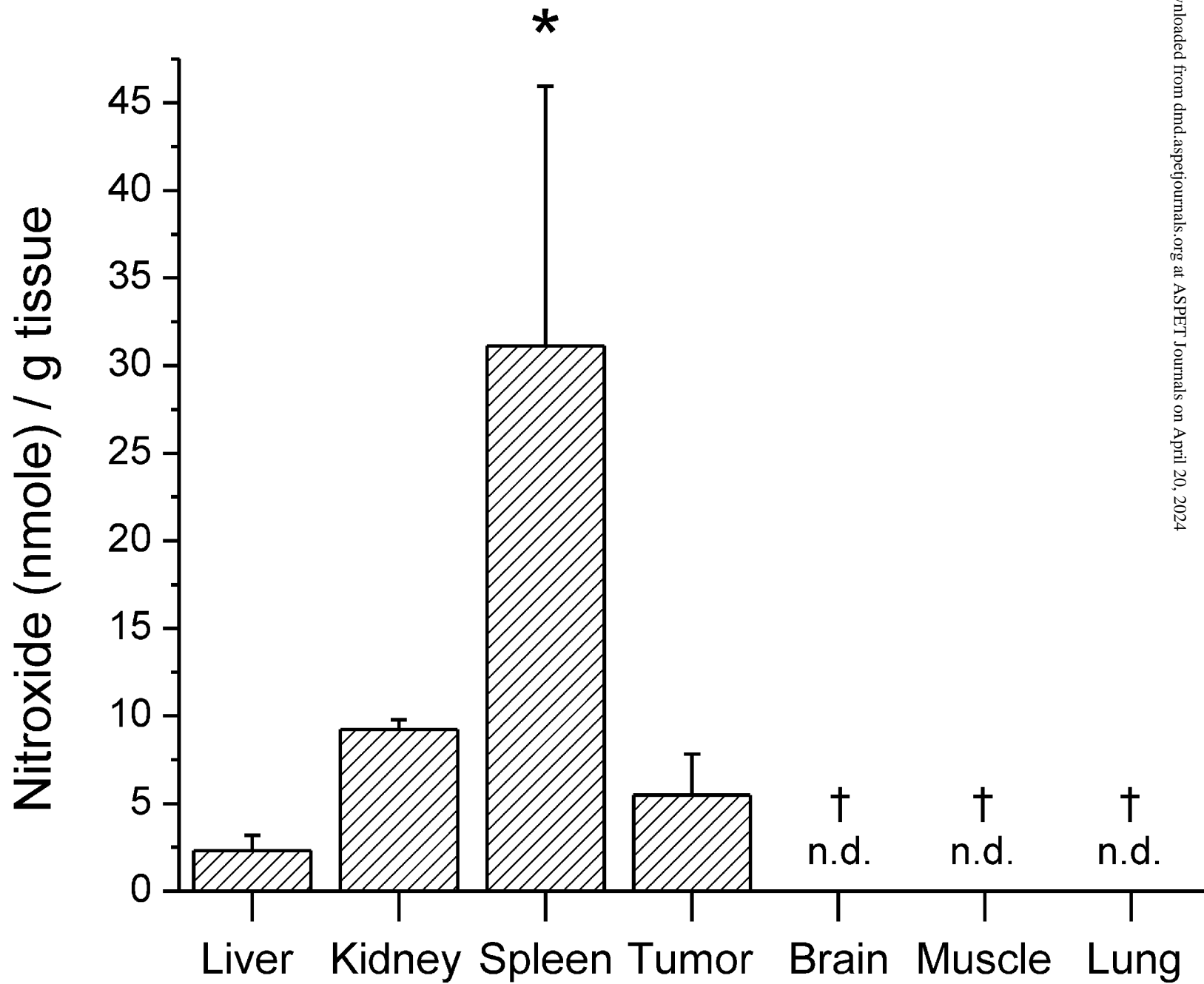


Figure 7

